

Available at www.sciencedirect.com

SciVerse ScienceDirect

journal homepage: www.elsevier.com/locate/carbon

Increased thermal conductivity of liquid paraffin-based suspensions in the presence of carbon nano-additives of various sizes and shapes

Zi-Tao Yu ^a, Xin Fang ^a, Li-Wu Fan ^{a,b,*}, Xiao Wang ^a, Yu-Qi Xiao ^a,
Yi Zeng ^a, Xu Xu ^c, Ya-Cai Hu ^a, Ke-Fa Cen ^b

^a Institute of Thermal Science and Power Systems, Department of Energy Engineering, Zhejiang University, Hangzhou 310027, PR China

^b State Key Laboratory of Clean Energy Utilization, Department of Energy Engineering, Zhejiang University, Hangzhou 310027, PR China

^c Institute of Energy Engineering, College of Metrological and Measurement Engineering, China Jiliang University, Hangzhou 310018, PR China

ARTICLE INFO

Article history:

Received 26 July 2012

Accepted 27 October 2012

Available online xxxx

ABSTRACT

The effect of adding carbon nanomaterials on the thermal conductivity of liquid paraffin-based suspensions was investigated. These included pristine and carboxyl-functionalized short multi-walled carbon nanotubes (MWCNTs), long MWCNTs, carbon nanofibers, and graphene nanoplatelets (GNPs). The thermal conductivity of the suspensions was measured using the transient hot-wire method at a constant temperature. The size, shape, and dispersion of the carbon additives were observed by microscopy, and the stability and viscosity of the suspensions were also characterized. It was shown that thermal conductivity of the suspensions increases with increasing the loading of the carbon additives and the extent of relative increase depends strongly on their size and shape. Of the various carbon nanomaterials examined, GNPs caused greatest increase due to reduced thermal interface resistance associated with their two-dimensional planar structure. The viscosity of GNP-based suspensions decreases at relatively high loadings, whereas a monotonic increase was observed for suspensions with all the other carbon additives.

© 2012 Elsevier Ltd. All rights reserved.

1. Introduction

The inclusion of highly-conductive particles to form suspensions/composites is a straightforward and promising approach to increasing thermal conductivity of the matrix materials. This technique has been attempted and practiced for many decades with meso- to micro-scale additives, and has recently turned to the use of emerging nanometer-sized candidates due to size effect-related advantages offered by such ultrafine materials. Utilization of engineered nanoparticle suspensions for heat transfer applications, coined as nanofluids [1], has been the subject of tremendous archived

publications in the past decade. Of the various highly-conductive nanostructures available, the family of carbon nanomaterials has attracted increasing attention due to their superior thermal conductivity (of the order of 1000 W/mK) over the conventional metal, oxide, and ceramic nanoparticles. Therefore, although in a recent benchmark study the increased thermal conductivity of nanofluids with conventional nanoparticles was found experimentally to agree fairly well with that predicted by the Maxwell's equation [2], far more remarkable increase has been realized for carbon additives, including carbon nanotubes (CNTs) [3], graphite nanoparticles [4], and emerging graphene nanomaterials [5–12].

* Corresponding author. Fax: +86 571 87952378.

E-mail address: liwufan@gmail.com (L.-W. Fan).

0008-6223/\$ - see front matter © 2012 Elsevier Ltd. All rights reserved.

<http://dx.doi.org/10.1016/j.carbon.2012.10.059>

The functionality of nanofluids has recently been extended to nano-enhanced phase change materials (NePCMs) that will undergo cyclic solid–liquid phase change for latent heat (of fusion) thermal energy storage [13]. The NePCMs may be considered as custom PCMs that possess higher thermal conductivities than those of the matrix PCMs. This idea has added a new dimension to the research of thermal conductivity increase of PCMs that was centered on the use of meso-scale extended surfaces, e.g., metal fins/foams [14]. Not surprisingly, carbon nanomaterials, such as CNTs and carbon nanofibers (CNFs) [15–18] and graphene/graphite nanoplatelets (GNPs) [19,20], have been the favorable additives for NePCMs. The aforementioned efforts have been primarily dedicated to thermal conductivity measurements of NePCMs in the solid phase. While being operated in the liquid phase, NePCMs can be considered as nanofluids based on liquid PCMs. In the available literature, however, attention has rarely been paid to thermal conductance characterization of liquid NePCMs. Furthermore, in addition to the loading, thermal conductivity increase of nanofluids/NePCMs has shown to depend strongly on a variety of physical and chemical properties of the additives, such as size, shape, agglomeration, and chemical functionalization, and these complicated factors have led to significant uncertainty in the measured thermal conductivity data.

In order to extend the existing knowledge, this paper will attempt to compare the potential among carbon nanomaterials of various sizes and shapes in serving as the additives for suspensions, with an emphasis on the emerging graphene nanomaterials. Experimental measurements of the increased thermal conductivity of paraffin-based suspensions (i.e., paraffin-based NePCMs in the liquid phase) will be performed. The stability and viscosity of the suspensions will also be examined to give a more general basis of comparison.

2. Experimental

2.1. Materials and sample preparation

Paraffin wax is a family of alkane mixtures that are widely used in thermal energy storage applications for the low-to-medium temperature range, e.g., solar water heating and thermal management of electronics. In this study, a paraffin (supplied by Sinopharm Chemical Reagent Co., Ltd) with a nominal melting temperature of 58–60 °C was chosen as the base PCM. The various carbon nanomaterials involved were pristine and carboxyl-functionalized short multi-walled CNTs (MWCNTs), long MWCNTs, CNFs, and GNPs, with the 3 types of CNTs being hereafter coined as S-MWCNTs, C-S-MWCNTs,

and L-MWCNTs, respectively. The suppliers and the given specifications of these 5 carbon additives are listed in Table 1.

In order not to complicate the analysis of thermal conductivity increase, the carbon nanomaterials were used as received without further functionalization or adding any surfactants/dispersants. It is noted that the C-S-MWCNTs were already functionalized by carboxylic groups. A two-step protocol was followed to prepare the suspension samples, as illustrated in Fig. 1.

Paraffin was pre-melted and degassed in a vacuum oven for 3 h at 110 °C before use. Carbon nanomaterials were then poured into the molten paraffin to form suspensions. Dispersion of the additives was accomplished by shear mixing (magnetic stirrer) for 15 min, followed by bath sonication (40 kHz, 200 W) for 50 min. During these operations, temperature of the samples was kept at 75 °C. For each kind of carbon additives, 4 samples with a mass fraction (ϕ_{wt}) ranging from 1 to 4 wt.% at an increment of 1 wt.% were prepared. A sample of pure liquid paraffin (0 wt.%) was also prepared to serve as the baseline case for comparison. Therefore, there were a total of 21 samples to be characterized.

2.2. Microscopic characterization

In order to verify the actual size and shape of the carbon nanomaterials utilized, the scanning electron microscopy (SEM) technique was employed. The imaging was performed on a Hitachi SU-70 high resolution field emission SEM for the nanomaterials as received. Due to their desirably high electrical conductance, the SEM images were taken directly on carbon nanomaterial samples without gold coating. In addition, by utilizing the atomic force microscopy (AFM) technique, performed on a Veeco MultiMode AFM under tapping mode, the surface morphology and thickness of the GNPs were also measured.

On the other hand, the size and distribution of the carbon nanomaterials after being dispersed into liquid paraffin were examined by utilizing both transmission electron microscopy (TEM) and dynamic light scattering (DLS) techniques. The TEM imaging of the liquid samples was performed on a JEOL JEM-1230 instrument under pendent-drop mode. The DLS characterization was performed on a Malvern Zetasizer Nano S90 to determine the equivalent hydrodynamic diameters representing the clustering sizes of the carbon additives (treated as spheres) in fresh samples.

2.3. Transport property measurements

Thermal conductivity measurements of the suspensions were performed on a KD2 Pro instrument that is based on the tran-

Table 1 – Suppliers and given specifications of the various carbon nanomaterials adopted in the present study.

Material	Supplier	Dimensions	Purity (wt.%)
S-MWCNTs	Chengdu Organic Chemicals Co. Ltd.	Length: 0.5–2 μm , diameter: 8–15 nm	>95
C-S-MWCNTs	Chengdu Organic Chemicals Co. Ltd.	Length: 0.5–2 μm , diameter: 8–15 nm	>95
L-MWCNTs	Shenzhen Nanotech Port Co. Ltd.	Length: 5–15 μm , diameter: <10 nm	>97
CNFs	Chengdu Organic Chemicals Co. Ltd.	Length: 10–30 μm , diameter: 150–200 nm	>95
GNPs	Chengdu Organic Chemicals Co. Ltd.	Diameter: 5–10 μm , thickness: 4–20 nm	>99

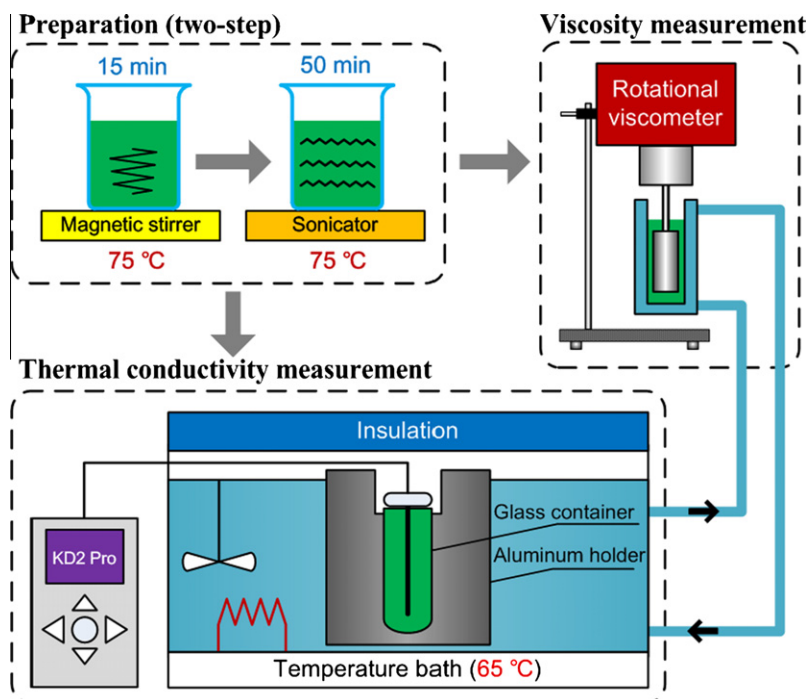


Fig. 1 – Diagram of the experimental procedure and set-up for sample preparation and transport property measurements.

sient hot-wire (THW) method, which has 3 sensors for measuring various types of materials with a general accuracy of 5%. As recommended by the manufacturer (Decagon Devices), the KS-1 sensor (length: 6 cm, diameter: 1.27 mm) was used for liquids. For precisely controlling the measurement temperature, a temperature bath/circulator (Brookfield TC-502P) with a stability of 0.01 °C was utilized. During measurements, the samples (in liquid phase) were held in a custom cylindrical container (length: 8 cm, inner diameter: 1 cm) made of Pyrex glass having a thermal conductivity of approximately 1 W/mK. The glass container was inserted into a holder made of aluminum (237 W/mK). This aluminum holder was submerged in the temperature bath to serve as an isothermal bulk for assuring temperature uniformity in the samples, as sketched in Fig. 1. Thermal equilibrium between the samples and the bath was assured by waiting for a sufficiently long time (more than 15 min) after the bath temperature had reached the set point. Temperature variations in the samples were monitored using a type-K thermocouple (calibrated to have an uncertainty of 0.3 °C). The accuracy and reproducibility of the THW instrument were verified with ethylene glycol at elevated temperatures before use.

The dynamic viscosity of the suspensions was measured using a rotational viscometer (Brookfield DV-C) with the aid of an adaptor for liquids with low viscosities. The aforementioned temperature bath/circulator was used again by connecting with the water-cooled jacket of the adaptor, in an effort to control the temperature of the samples held in the adaptor, as illustrated in Fig. 1. Before viscosity measurements, the type-K thermocouple was again used to assure thermal equilibrium between the samples and the circulator. The accuracy and reproducibility of the viscometer were also assured by conducting measurements with a standard liquid of precisely known viscosity.

It is noted that other than the above-mentioned 21 samples, various test samples from different batches of suspensions with the highest loading of 4 wt.% of all the carbon additives were also tested before measurements for inspecting the dependence of the measured thermal transport property data on uniqueness of the samples. It was found that spreading of the data was very small with a standard deviation of less than 3.3% that is within the specified uncertainty of the instruments (5%), as long as the measurements were completed on fresh samples (before precipitation). After performing the tests, a confidence was established on the reproducibility of the measurements on multiple samples. Hence, the following measurements were only performed on a single sample for each case.

3. Results and discussion

3.1. Dispersion of the carbon additives and stability of the suspensions

The SEM images of the carbon nanomaterials as received are presented in Fig. 2. Looking through Fig. 2a–d, it is obvious that the CNTs and CNFs were all thin-wire-shaped with increasing length and diameter. The diameters for S-MWCNTs, C-S-MWCNTs, L-MWCNTs, and CNFs were determined to be roughly 20, 20, 40, and 100 nm, respectively.

The GNPs, however, possessed a planar geometry with high size-to-thickness aspect ratios and the SEM image (see Fig. 2e) can only demonstrate their size (>1 μm). As illustrated in Fig. 2f, the thickness of a typical well-isolated GNP was nearly 78 nm, which consisted of approximately 230 layers of monolayer graphene (interlayer spacing is 0.335 nm). The aspect ratio of this individual GNP was about 200. Because it

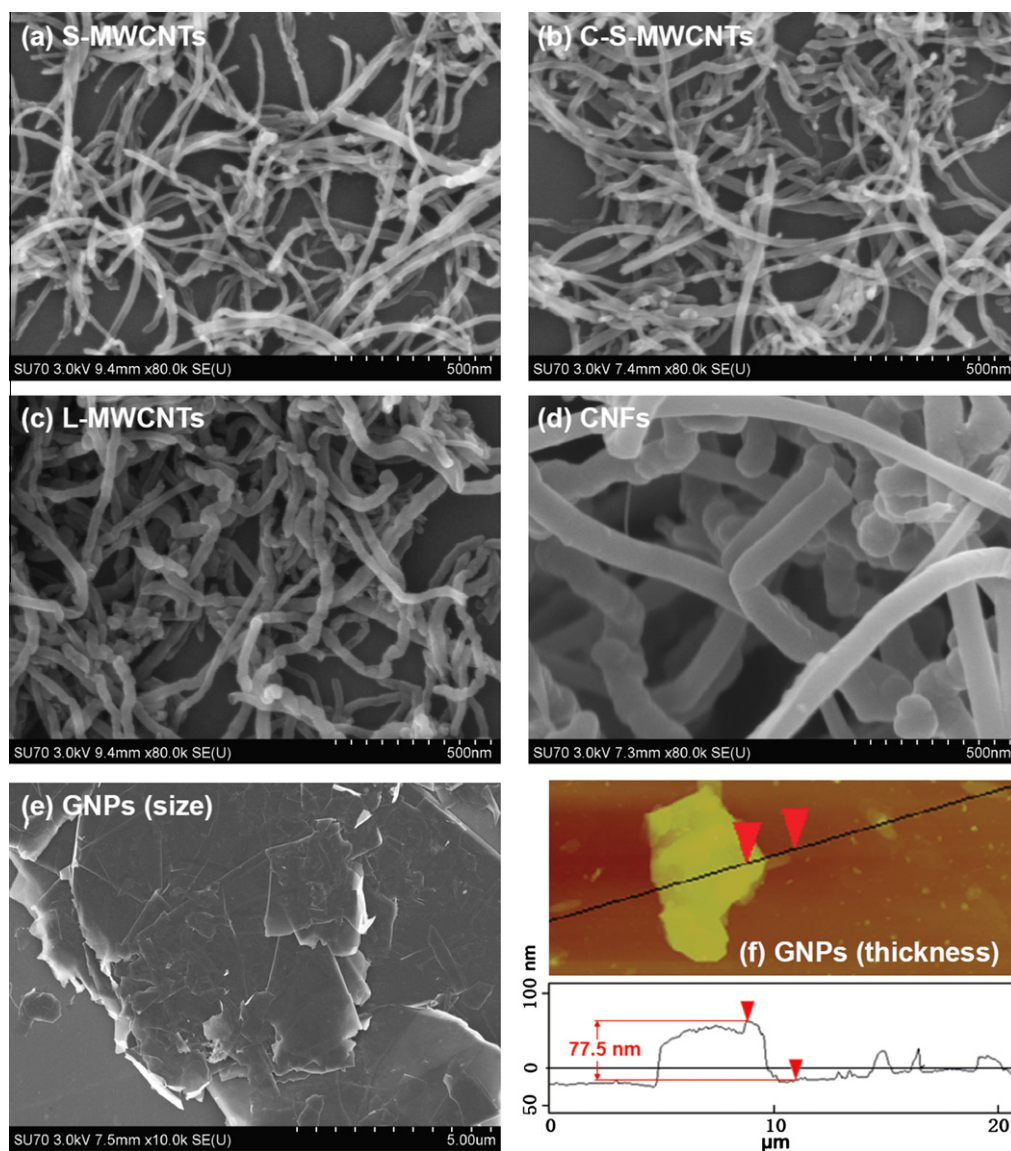


Fig. 2 – Sizes and shapes of the carbon nanomaterials as-received characterized by SEM images of (a) S-MWCNTs, (b) C-S-MWCNTs, (c) L-MWCNTs, (d) CNFs, (e) GNPs (size), and by AFM image of (f) an individual GNP (thickness).

was hard to define the size for GNPs with an irregular shape, the size was roughly determined by measuring the maximum distance between two arbitrary points along the boundary of GNPs based on the microscopic images. Generally, the measured sizes of the carbon nanomaterials were somewhat larger than those specified by the suppliers (see Table 1), indicating that agglomeration/clustering had happened in the materials received.

As presented in Fig. 3, the sizes of the carbon nanomaterials observed previously by the SEM images are confirmed by the TEM images. The two shortest carbon additives, S-MWCNTs and C-S-MWCNTs, are shown to have desirable dispersion with insignificant agglomeration. The dispersion, however, became worse as the size of the carbon additives increases. A typical clustering size of L-MWCNTs of 1.5 μm is shown in Fig. 3c and the agglomeration effect of CNFs and GNPs became even more pronounced due to their intrinsically large sizes. As shown in Fig. 3f, the nominal average diam-

eters obtained by the DLS technique are in good agreement with the agglomeration sizes determined via the TEM images (see Fig. 3a–e). The increase of the nominal diameter is clearly seen with the smallest (for S-MWCNTs and C-S-MWCNTs) and greatest (for GNPs) values being nearly 1 and 3 μm , respectively.

Although the dispersion of carbon additives in fresh samples has been examined quantitatively, long-term stability of the suspensions is still of great interest, which is not only the concern of practical applications, but is also important for reliable and reproducible measurements of transport properties. Visual observation was thus carried out on suspensions with the highest loading investigated (4 wt.%) at various time instants. All the 5 samples were observed to be stable after standing in jars for 1.5 h without visible precipitation, during which property measurements were able to be accomplished. The sample with GNPs became the visually most unstable one after 1 day and it was found that the stability of the suspen-

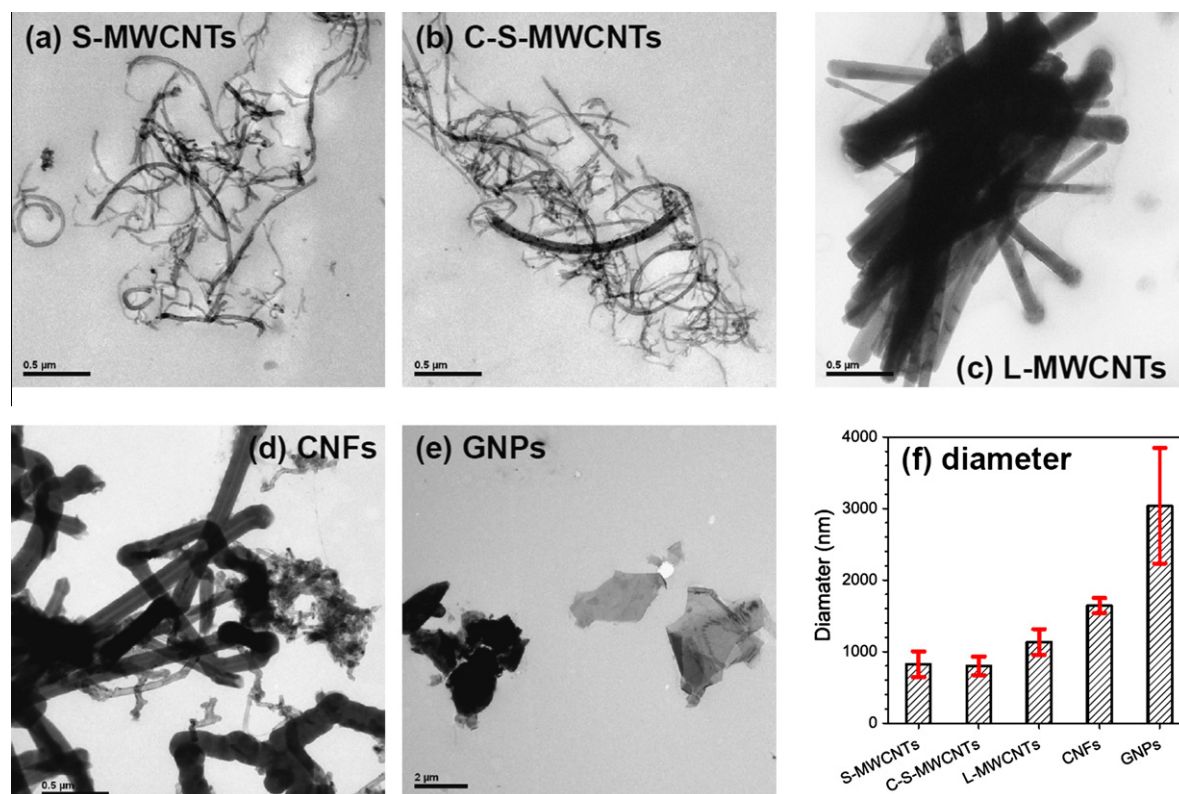


Fig. 3 – Agglomerations of the carbon nanomaterials after dispersion represented by TEM images of (a) S-MWCNTs, (b) C-S-MWCNTs, (c) L-MWCNTs, (d) CNFs, and (e) GNPs, and (f) comparison of nominal clustering size distributions determined by the DLS technique.

sions became worse with increasing clustering size of the carbon additives. It is noted that the stability test was performed on samples with the highest loading of 4 wt.%, i.e., the most rigorous case. For samples with lower concentrations, better long-term stability may be expected.

3.2. Increased thermal conductivity and viscosity: effects of size and shape of the carbon additives

Thermal conductivity measurements were performed for the liquid paraffin-based suspensions at 65 °C. For each sample, measurement was repeated for 5 times and all the data presented herein are the average values with a standard deviation less than 1%. The measured thermal conductivity of the suspensions as a function of the loading of the carbon additives is presented in Fig. 4.

The thermal conductivity of pure paraffin at 65 °C was determined to be $k_0 = 0.1504$ W/mK. As compared to this baseline value, thermal conductivity of the suspensions increased almost linearly with increasing the loading of each carbon additive. The extent of relative increase, however, was clearly distinct among the various carbon additives. The suspensions with L-MWCNTs demonstrate marginal increase that the absolute value of thermal conductivity was only increased by 0.012 W/mK for the highest loading of 4 wt.%. In addition, although a recent study postulated and verified that clustering of the additives dominates heat conduction in nanofluids [21], the clustering size is not shown

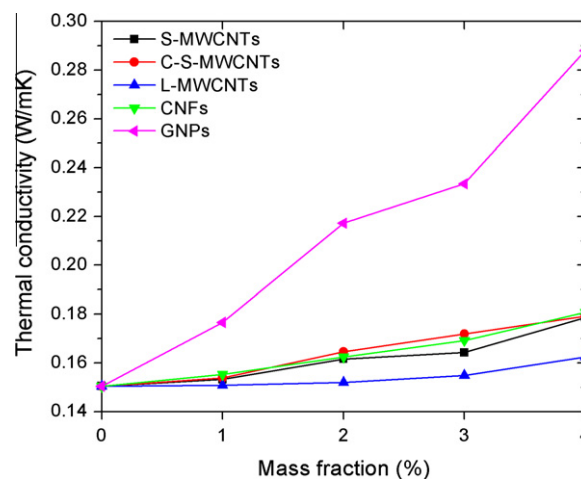


Fig. 4 – Measured thermal conductivity of the liquid paraffin-based suspensions as a function of the loading of various carbon additives.

to have monotonic influence in the present work. The S-MWCNTs, C-S-MWCNTs, and CNFs caused similar level of increase, which is more significant than that of the L-MWCNT samples with the greatest absolute increases being slightly above 0.03 W/mK at 4 wt.% loading, i.e., relatively increased by about 20%. The functionalization on MWCNTs with carboxylic groups has insignificant effect on their performance in thermal conductivity increase.

The planar GNPs, however, remarkably outperformed in thermal conductivity increase over their wire-shaped counterparts, as shown in Fig. 4. For the sample with 4 wt.% GNPs, the thermal conductivity was determined to be as high as 0.29 W/mK, which is nearly double that of pure paraffin. That is, a nearly 100% thermal conductivity increase of liquid paraffin was achieved by adding only 4 wt.% GNPs. Because the thermal conductivities of GNPs and CNTs/CNFs have been reported to possess similar values (~ 3000 W/mK), this outperformance is likely attributed to the particular two-dimensional planar morphology of GNPs that leads to larger contact area, and in turn smaller thermal interface resistance, between the additives and matrix materials. Similar outperformance of GNPs was reported by Yu et al. [22] for epoxy-based nanocomposites (in solid phase) over various carbon fillers including single-walled CNTs, graphite micro-particles, and carbon black. The reduced geometric contribution to phonon mismatch-induced phonon scattering at the interfaces was interpreted to be responsible for the low thermal interface resistance offered by GNPs [22].

On the other hand, the presence of additives would increase the viscosity of a fluid, which has been considered one of the most serious problems of the utilization of nanofluids [23]. In the present study, viscosity of the paraffin-based suspensions was also measured at 65 °C. The baseline value, i.e., the viscosity of pure paraffin, was determined to be 5.892 mPa s. The loading dependence of the measured viscosity of the suspensions is presented in Fig. 5, in which the vertical axis is logarithmic.

It is shown that viscosity of the suspensions with S-MWCNTs and C-S-MWCNTs increases significantly while elevating their loading. The greatest value exceeded 800 mPa s for the 4 wt.% samples, i.e., more than 140 times greater than that of the pure paraffin. Similar to that observed for thermal conductivity, the carboxyl-functionalization is also shown to have negligible influence on viscosity of the suspensions. As the size of the carbon additives increases, the extent of viscosity increase was greatly suppressed. For the suspensions with L-MWCNTs and CNFs, the viscosity at 4 wt.% was deter-

mined to be only 40 mPa s, an order of magnitude lower than that of the S-MWCNT suspension.

As shown in Fig. 5, an interesting phenomenon is seen for the GNP-based suspensions that the loading dependence of viscosity is not monotonic with a critical point being found at 2 wt.%. The viscosity initially increases as more GNPs were introduced and the relative increase is similar to those of the suspensions with L-MWCNTs and CNFs. Beyond this critical point, however, a reverse tendency occurs that the viscosity decreases with increasing the loading. At the highest loading of 4 wt.%, the viscosity of the GNP-based suspension was only 11.5 mPa s, which is less than twice over the baseline value. The decrease of viscosity at higher loadings is possibly due to shear-induced alignment and inter-sliding of the planar GNP flakes along the concentric streamlines during viscosity measurements. Obviously, this is a favorable plus for GNPs to stand out among various carbon nanomaterials for thermal conductivity increase of engineered suspensions.

3.3. Comparison of thermal conductivity increase of suspensions (nanofluids) due to graphene nanomaterials

Having shown that the GNPs, primarily due to their particular planar shape, outperform the other carbon nanomaterials for both the superior potential in thermal conductivity increase and the lowest penalty for increased viscosity, a fact is realized that the actual performance in practical applications would be complicated as the size and aspect ratio of GNPs vary significantly. The GNPs utilized in the present work had dimensions close to those of the GNPs exfoliated at 200 °C in Yu et al. [22], referred to as GNP-200. As compared to GNPs exfoliated at higher temperatures (400 and 800 °C) in that work, GNP-200 possessed the greatest thickness, where the other two thinner GNPs were shown to have slightly better performance in thermal conductivity increase [22]. In the present work, it was unable to compare among various GNPs with different sizes and aspect ratios due to the availability. A comparison of the present results with previous studies concerning graphene-based nanofluids with an emphasis on increased thermal conductivity [5–12] is therefore made in an effort to further justify the better performance of graphene nanomaterials over other carbon additives by excluding the possible cause of uniqueness of the samples, in considering the great uncertainty associated with the materials, sample preparation, and thermal conductivity measurement methods adopted.

The specifications of the various graphene nanomaterials utilized in these studies are listed in Table 2. The graphene oxide nanosheets (GONs) and graphene nanosheets (GNSs) synthesized by Yu et al. [5,6,8] using a modified Hummers method were claimed to have a thickness around 1 nm (about 2–4 layers of graphene), much thinner than the GNPs used in the present work. In addition, as listed in Table 3, the base liquids investigated in these studies were mostly polar (water and ethylene glycol) and the thermal conductivity was measured at elevated temperatures. Therefore, a direct comparison of the present results with those reported in the literature is made by means of the relative thermal conductivity increase, defined as $k - k_0/k_0$, as shown in Fig. 6a. It is noted that only the data measured at the respective lower tempera-

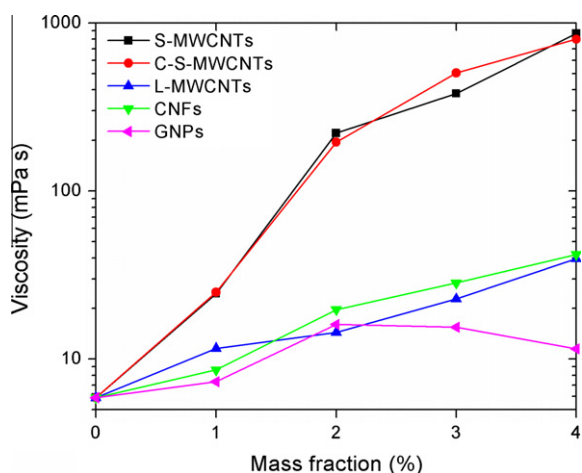


Fig. 5 – Measured dynamic viscosity of the liquid paraffin-based suspensions as a function of the loading of various carbon additives.

Table 2 – Specifications of the graphene nanomaterials utilized in relevant studies concerning graphene-based nanofluids.

Reference	Material	Synthesis method	Surfactant	Dimensions		Loading
				Size	Thickness	
Yu et al. [5]	GONs ^a	Modified Hummers method	N/A	1–3 μm	0.8–1.2 nm	1–5 vol%
Yu et al. [6]	GONs	Modified Hummers method	Oleylamine	0.5–3 μm	0.6–1.1 nm	1–5 vol%
Baby and Ramaprabhu [7]	GNSs ^b	Hummers method	N/A	N/A	N/A	0.005–0.0056 vol%
Yu et al. [8]	GNSs	Modified Hummers method	SDBS ^c	0.2–2 μm	0.7–1.3 nm	1–5 vol%
Baby and Ramaprabhu [9]	GNSs coated with silver nanoparticles	Hummers method	N/A	N/A	N/A	0.005–0.07 vol%
Baby and Ramaprabhu [10]	GNSs coated with copper nanoparticles	Hummers method	N/A	N/A	N/A	0.005–0.07 vol%
Gupta et al. [11]	GNSs	Hummers method	N/A	5 nm–1.5 μm	N/A	0.01–0.2 vol%
Martin-Gallego et al. [12]	GNSs	Brodie method	N/A	N/A	N/A	1 wt. %

^a GONs denote graphene oxide nanosheets.
^b GNSs denote graphene nanosheets.
^c SDBS denotes sodium dodecylbenzenesulfonate.

Table 3 – Matrix materials and characterization techniques adopted in relevant studies concerning graphene-based nanofluids.

Reference	Base liquid	Stability concern	TC ^a measurement	Temperature (°C)
Yu et al. [5]	Ethylene glycol	Stability quantified after 2 months by monitoring the variation of UV–Vis ^b absorption intensity	Custom THW	10–60
Yu et al. [6]	Distilled water, propyl glycol, and liquid paraffin	Long-term stability claimed	Custom THW	10–60
Baby and Ramaprabhu [7]	Water and ethylene glycol	Long-term stability claimed	KD2 Pro	25–50
Yu et al. [8]	Ethylene glycol	Stability claimed	Custom THW	10–60
Baby and Ramaprabhu [9]	Deionized water and ethylene glycol	Stability quantified after 2 months by monitoring the settling of particles via visual observation	KD2 Pro	25–70
Baby and Ramaprabhu [10]	Water and ethylene glycol	N/A	KD2 Pro	25–50
Gupta et al. [11]	Water	Stability claimed for more than 6 months	Custom THW	30–50
Martin-Gallego et al. [12]	Liquid epoxy resin (bisphenol A diglycidyl ether)	N/A	KD2 Pro	30–60

^a TC stands for thermal conductivity.
^b UV–Vis stands for ultraviolet-visible spectroscopy.

ture limits are collected from the literature and the mass fraction of the present results is converted into volume fraction by assuming a nominal density of 2620 kg/m³ for GNPs [6]. Moreover, the results in Refs. [7,10,12] are excluded since the baseline values were not available.

It is shown that the “thick” GNPs in the present work lead to greater increase than those realized by the much thinner GONs/GNSs in Yu et al. [5,6,8]. This anomalous phenomenon may be resulted from clustering of the GONs/GNSs after dispersion, although these materials were claimed to be ultra thin as synthesized. The data obtained by Gupta et al. [11]

are in good agreement with the present work, whereas Baby and Ramaprabhu [9] reported extremely high increase at dilute concentrations (<0.1 vol.%), possibly due to coating of silver nanoparticles on the graphene nanostructures that further lowers the thermal interface resistance. The thickness and clustering state of the graphene nanomaterials examined, however, were not mentioned in these two studies [9,11].

Inspired by Gharagozloo et al. [24], a figure of merit, defined by $k - k_0/(k_0\phi_{vol})$ with ϕ_{vol} being the volume fraction, is introduced to describe quantitatively the potential of an addi-

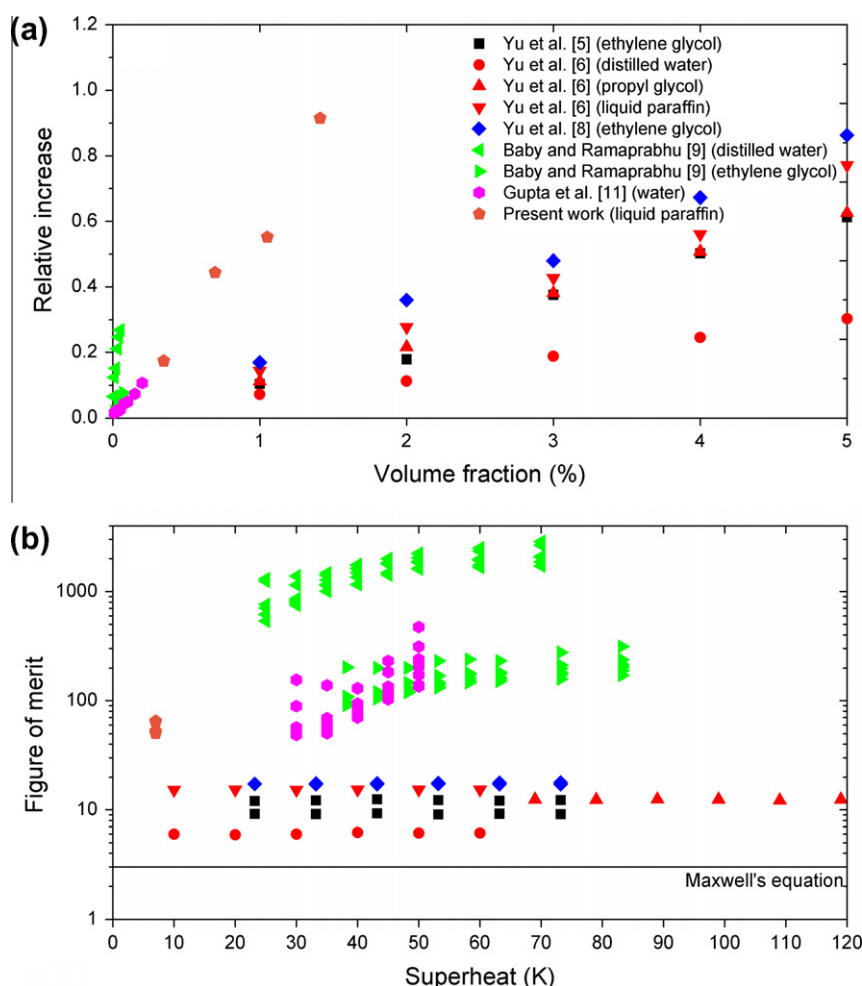


Fig. 6 – Comparison of the (a) relative thermal conductivity increase and (b) figure of merit in nanoparticle suspensions (nanofluids) consisting of various base liquids and graphene nanomaterials.

tive in thermal conductivity increase. For the data collected at widely spreading loadings, this figure of merit is a unified means for comparison. Fig. 6b presents the figure of merit as a function of superheat, defined as the difference between the measurement temperature and the melting temperature of the base liquid, in which all the available temperature-dependent data points in the literature are involved. It is clearly shown that all the examined combinations of graphene nanomaterials and base liquids lead to a figure of merit far beyond 3, which is the theoretical value predicted by the Maxwell's equation [2], and that it is almost independent of the measurement temperature. The figure of merit of the present results was found to be around a moderate value of 60, while the results presented by Yu et al. [5,6,8] were around 10 and the values exceed 1000 for the silver nanoparticle-coated graphene in distilled water [9]. It is expected that by reducing the size (i.e., physical manipulation) and chemical functionalization, which may facilitate phonon transfer so as to decrease the thermal interface resistance, the potential of GNPs in thermal conductivity increase may be further tapped.

Furthermore, the hydrophilic nature of graphene allows it to have desirable dispersion in polar solvents without the aid

of any surfactants [6]. While being dispersed in non-polar liquids, e.g., liquid paraffin, a surfactant is required for graphene nanomaterials, e.g., the oleylamine adopted by Yu et al. [6]. The suspensions would otherwise be rather unstable. Therefore, the stability issue must be addressed for such a promising additive material. It is also expected that regulation of the transport properties of graphene-based suspensions would become more complicated in the presence of surfactants.

4. Conclusions

Experimental measurements of thermal conductivity and viscosity of liquid paraffin-based suspensions with carbon nano-additives of various sizes and shapes have been presented in the present paper. It was shown that the GNPs, owing to their particular two-dimensional planar structure, have much greater potential in thermal conductivity increase than that of the other wire-shaped carbon nanomaterials, i.e., CNTs and CNFs. This was elucidated to result from the reduced geometric contribution of phonon scattering at the interfaces between planar GNPs and matrix material. On the other hand, the use of GNPs led to the lightest penalty of viscosity increase with the viscosity being found to even decrease at rel-

atively high loadings. These advantages clearly identify graphene nanomaterials as a favorable additive for thermal conductivity increase of suspensions.

Hence, the GNP-based paraffin suspensions may be considered as a promising custom PCM for thermal energy storage systems, including passive thermal management of buildings, batteries, and electronics, with greatly enhanced capability of thermal responses. However, the GNP-based suspensions were shown to be unstable without adding any surfactants. Therefore, further efforts will be required to address the stability issue by manipulating physically and/or chemically the graphene nanomaterials, which would in turn affect, or may allow active control of, the performance of such materials in serving as additives for engineered suspensions.

Acknowledgements

This material is based upon work supported by the National Natural Science Foundation of China (NSFC) under Grant nos. 51276159 and 51106144, and China Postdoctoral Science Foundation (CPSF) under Grant no. 2012M511362. Thanks are due to Mr. Hua Wang, Ms. Jingping Zhu, and Ms. Na Zheng of the Center of Analysis and Measurement in the Faculty of Agricultural, Life and Environmental Sciences, the Center of Electron Microscope in the Department of Materials Science and Engineering, and the Department of Chemical and Biological Engineering, respectively, at Zhejiang University for their assistance in obtaining microscopy images.

REFERENCES

- [1] Das SK, Choi SUS, Yu W, Pradeep T. Nanofluids: science and technology. Hoboken (NJ): John Wiley and Sons; 2008.
- [2] Buongiorno J, Venerus DC, Prabhat N, McKrell T, Townsend J, Christianson R, et al. A benchmark study on the thermal conductivity of nanofluids. *J Appl Phys* 2009;106(9):094312.
- [3] Xie H, Lee H, Youn W, Choi M. Nanofluids containing multiwalled carbon nanotubes and their enhanced thermal conductivities. *J Appl Phys* 2003;94(8):4967–71.
- [4] Zhu H, Zhang C, Tang Y, Wang J, Ren B, Yin Y. Preparation and thermal conductivity of suspensions of graphite nanoparticles. *Carbon* 2007;45(1):226–8.
- [5] Yu W, Xie H, Bao D. Enhanced thermal conductivities of nanofluids containing graphene oxide nanosheets. *Nanotechnology* 2010;21(5):055705.
- [6] Yu W, Xie H, Chen W. Experimental investigation on thermal conductivity of nanofluids containing graphene oxide nanosheets. *J Appl Phys* 2010;107(9):094317.
- [7] Baby TT, Ramaprabhu S. Investigation of thermal and electrical conductivity of graphene based nanofluids. *J Appl Phys* 2010;108(12):124308.
- [8] Yu W, Xie H, Wang X, Wang X. Significant thermal conductivity enhancement for nanofluids containing graphene nanosheets. *Phys Lett A* 2011;375(10):1323–8.
- [9] Baby TT, Ramaprabhu S. Synthesis and nanofluid application of silver nanoparticles decorated graphene. *J Mater Chem* 2011;21(26):9702–9.
- [10] Baby TT, Ramaprabhu S. Synthesis and transport properties of metal oxide decorated graphene dispersed nanofluids. *J Phys Chem C* 2011;115(17):8527–33.
- [11] Gupta SS, Siva VM, Krishnan S, Sreeprasad TS, Singh PK, Pradeep T, et al. Thermal conductivity enhancement of nanofluids containing graphene nanosheets. *J Appl Phys* 2011;110(8):084302.
- [12] Martin-Gallego M, Verdejo R, Khayet M, Ortiz de Zarate JM, Essalhi M, Lopez-Manchado MA. Thermal conductivity of carbon nanotubes and graphene in epoxy nanofluids and nanocomposites. *Nano Res Lett* 2011;6:610.
- [13] Hosseineizadeh SF, Khodadadi JM. Nanoparticle-enhanced phase change materials (NEPCM) with great potential for improved thermal energy storage. *Int Commun Heat Mass Tran* 2007;34(5):345–54.
- [14] Fan L, Khodadadi JM. Thermal conductivity enhancement of phase change materials for thermal energy storage: a review. *Renew Sustain Energy Rev* 2011;15(1):24–46.
- [15] Elgafy A, Lafdi K. Effect of carbon nanofiber additives on thermal behavior of phase change materials. *Carbon* 2005;43(15):3067–74.
- [16] Zeng JL, Cao Z, Yang DW, Xu F, Sun LX, Zhang XF, et al. Effects of MWNTs on phase change enthalpy and thermal conductivity of a solid–liquid organic PCM. *J Therm Anal Calorim* 2009;95(2):507–12.
- [17] Wang J, Xie H, Xin Z, Li Y. Increasing the thermal conductivity of palmitic acid by the addition of carbon nanotubes. *Carbon* 2010;48(14):3979–86.
- [18] Cui Y, Liu C, Hu S, Yu X. The experimental exploration of carbon nanofiber and carbon nanotube additives on thermal behavior of phase change materials. *Sol Energy Mater Sol Cells* 2011;95(4):1208–12.
- [19] Xiang J, Drzal LT. Investigation of exfoliated graphite nanoplatelets (xGnP) in improving thermal conductivity of paraffin wax-based phase change material. *Sol Energy Mater Sol Cells* 2011;95(7):1811–8.
- [20] Yavari F, Fard HR, Pashayi K, Rafiee MA, Zamiri A, Yu Z, et al. Enhanced thermal conductivity in a nanostructured phase change composite due to low concentration graphene additives. *J Phys Chem C* 2011;115(17):8753–8.
- [21] Gao JW, Zheng RT, Ohtani H, Zhu DS, Chen G. Experimental investigation of heat conduction mechanisms in nanofluids. Clue on Clustering. *Nano Lett* 2009;9(12):4128–32.
- [22] Yu A, Ramesh P, Itkis ME, Bekyarova E, Haddon RC. Graphite nanoplatelet-epoxy composite thermal interface materials. *J Phys Chem C* 2007;111(21):7565–9.
- [23] Venerus DC, Buongiorno J, Christianson R, Townsend J, Bang IC, Chen G, et al. Viscosity measurements on colloidal dispersions (nanofluids) for heat transfer applications. *Appl Rheol* 2010;20(4):44582.
- [24] Gharagozloo PE, Eaton JK, Goodson KE. Diffusion, aggregation, and the thermal conductivity of nanofluids. *Appl Phys Lett* 2008;93(10):103110.